

**MINERALOGY, PETROGRAPHY, AND OXYGEN ISOTOPIC COMPOSITIONS OF ULTRAREFRACTORY INCLUSIONS FROM CARBONACEOUS CHONDRITES.** A. N. Krot<sup>1\*</sup>, C. Ma<sup>2</sup>, K. Nagashima<sup>1</sup>, A. M. Davis<sup>3</sup>, J. R. Beckett<sup>2</sup>, S. B. Simon<sup>4</sup>, M. Komatsu<sup>5</sup>, T. J. Fagan<sup>5</sup>, F. Brenker<sup>6</sup>, M. A. Ivanova<sup>7</sup>, and A. Bischoff<sup>8</sup>. <sup>1</sup>University of Hawai'i, USA, \*[sasha@higp.hawaii.edu](mailto:sasha@higp.hawaii.edu); <sup>2</sup>California Institute of Technology, USA; <sup>3</sup>University of Chicago, USA. <sup>4</sup>University of New Mexico, USA; <sup>5</sup>Waseda University, Japan; <sup>6</sup>Goethe University, Germany; <sup>7</sup>Vernadsky Institute, Russia; <sup>8</sup>Institut für Planetologie, Germany.

**Introduction:** Ca,Al-rich inclusions (CAIs) with Group II rare earth element (REE) patterns, enriched in less refractory REEs (La, Ce, Pr, Nd, Sm, and Tm), are thought to have condensed from a gaseous reservoir from which more refractory REEs (Gd, Tb, Dy, Ho, Er and Lu) were removed. The carrier(s) of ultrarefractory (UR) REE patterns are still poorly known; hibonite, perovskite, and Zr,Sc-rich phases have been previously considered as potential candidates. Several newly discovered Zr-, Sc-rich minerals in CAIs are potential carriers of UR REE patterns. Systematic studies of oxygen-isotope compositions and REE patterns of such CAIs are scarce. Here we report on the mineralogy, petrology and O-isotope compositions of UR CAIs from CO, CV, CR, and CM carbonaceous chondrites (CCs).

**Analytical procedures:** The mineralogy and mineral chemistry of UR CAIs were studied with backscatter electron imaging (BSE), electron backscatter diffraction (EBSD), and electron probe microanalysis (EPMA) at CalTech and UH. Oxygen isotopes were measured with the UH Cameca ims-1280 ion microprobe in multicollection mode (FC-EM-EM) using a 15–20 pA Cs<sup>+</sup> primary beam focused to ~1 μm and rastered over 1×1 μm<sup>2</sup>. Instrumental mass fractionation (IMF) was corrected using Burma spinel (for Zr- and Sc-rich phases, hibonite, spinel, and perovskite), augite (davisite, Sc-pyroxenes, and Al-diopside), San Carlos olivine (for olivine, low-Ca pyroxene, and anorthite), and quartz (for quartz).

**Mineralogy and Petrography:** The UR CAIs are found in CVs, COs, CRs, CHs, and CMs, where they occur as (i) individual irregularly-shaped (nodular-like) inclusions, (ii) minor constituents of amoeboid olivine aggregates (AOAs) and Fluffy Type A CAIs, (iii) relict inclusions in coarse-grained igneous CAIs (forsterite-bearing Type Bs and compact Type As), and (iv) relict inclusions in chondrules [1–17; this study].

The UR CAIs studied are typically small, < 30 μm in size, and dominated by Zr, Sc, Ti, and Y-rich minerals, including warkite (Ca<sub>2</sub>Sc<sub>6</sub>Al<sub>6</sub>O<sub>20</sub>), davisite (CaScAlSiO<sub>6</sub>), Y-rich perovskite ((Ca,Y)TiO<sub>3</sub>), tazheranite ((Zr,Ti,Ca)O<sub>2-x</sub>), kangite ((Sc,Ti,Al,Zr,Mg,Ca,□)<sub>2</sub>O<sub>3</sub>), zirconolite CaZrTi<sub>2</sub>O<sub>7</sub>, eringaite Ca<sub>3</sub>(Sc,Y,Ti)<sub>2</sub>Si<sub>3</sub>O<sub>12</sub>, allendeite (Sc<sub>4</sub>Zr<sub>3</sub>O<sub>12</sub>), lakargite (CaZrO<sub>3</sub>), panguite ((Ti,Al,Sc,Mg,Zr,Ca)<sub>1.8</sub>O<sub>3</sub>), thortveitite (Sc<sub>2</sub>Si<sub>2</sub>O<sub>7</sub>), and machiite ((Al,Sc)<sub>2</sub>(Ti<sup>4+</sup>,Zr)<sub>3</sub>O<sub>9</sub>). These minerals are often associated with sub-μm grains of platinum group elements (PGEs: Ir, Os, Ru, Mo, and Wo). Most UR CAIs

appear to have escaped melting and are surrounded by Wark-Lovering (WL) rims of Sc-pyroxene, ±eringaite, Al-diopside, and ±forsterite. WL rims are absent around relict UR CAIs in igneous CAIs and chondrules, suggesting their destruction during melting.

**Oxygen isotopes:** On a three-isotope oxygen diagram, δ<sup>17</sup>O vs. δ<sup>18</sup>O, compositions of individual minerals from UR CAIs plot along ~slope-1 line. Note, however, since most minerals were analyzed without proper standards, the IMF effects cannot be properly corrected for; therefore, only mass-independent values, Δ<sup>17</sup>O = δ<sup>17</sup>O – 0.52×δ<sup>18</sup>O, are plotted in Fig. 1 and discussed below. Typical uncertainty on Δ<sup>17</sup>O is ~ 2.5‰ (2σ).

*UR CAIs in CCs of petrologic type ≤3.1.* Most UR CAIs from CCs of petrologic type ≤3.1 are isotopically uniform and have <sup>16</sup>O-rich compositions (Δ<sup>17</sup>O ~ –23‰). The Murchison UR CAI *MURI* composed of spinel, thortveitite, panguite, davisite, and Sc-rich diopside [8] may be uniformly <sup>16</sup>O-depleted: the only two minerals analyzed in this CAI, thortveitite and Sc-rich diopside, have Δ<sup>17</sup>O of ~ –8 to –5‰. There are 3 isotopically heterogeneous UR mineral-bearing objects: (1) #4 (circled number in Fig. 1), an intergrowth of <sup>16</sup>O-rich corundum (Δ<sup>17</sup>O ~ –24‰) with euhedral <sup>16</sup>O-poor machiite (Δ<sup>17</sup>O ~ 0‰) from Murchison [17], (2) #7, Sc-rich chondrule ZZ from MAC 88107 (CO3.1-like), and (3) #8, a relict hibonite-rich CAI in a type II chondrule (named by [18] as “FeO-rich fragment”) from Acfer 094 (C3.0 ungrouped). Chondrule ZZ consists of forsterite, Sc-bearing high-Ca and low-Ca pyroxenes, and baddeleyite, ± zirconolite. It may be an incompletely melted UR CAI-bearing AOA. Relict forsterite grains in this object retained <sup>16</sup>O-rich signature (Δ<sup>17</sup>O ≤ –17‰), whereas olivine, Sc-bearing high-Ca and low-Ca pyroxenes, which appear to have crystallized from chondrule melt, have <sup>16</sup>O-depleted compositions (Δ<sup>17</sup>O range from –5 to –4‰, from –4 to –2‰, and from –3 to 0‰, respectively), suggesting gas-melt isotope exchange during melt crystallization. The relict CAI from Acfer 094 consists of hibonite overgrown by Fe,Cr-bearing spinel; hibonite contains inclusions of zirconolite, tazheranite, perovskite, loveringite (Ca(Ti,Fe,Cr,Mg)<sub>21</sub>O<sub>38</sub>), and PGEs.

*UR CAIs in CCs of petrologic type ≥3.1.* Most UR CAIs in CCs of petrologic type ≥3.1 are isotopically heterogeneous. The isotopic heterogeneity appears to correlate with the mineralogy rather than with the inferred

crystallization sequence of individual CAIs. For example, spinel and hibonite of the CAI cores, and Al-diopside and forsterite of the WL rims are always  $^{16}\text{O}$ -rich, whereas other minerals are  $^{16}\text{O}$ -depleted to various degrees. The Allende UR CAI *Al-2* (#9) is an important exception. It consists of eringaite, spinel, perovskite, and davisite, and is a relict inclusion enclosed by a massive Al-diopside of the host forsterite-bearing CAI. The relict UR CAI shows a relatively small degree of isotope heterogeneity ( $\Delta^{17}\text{O} \sim -25$  to  $-19\%$ ), with spinel being slightly  $^{16}\text{O}$ -enriched relative to other minerals; spinel is isotopically similar to Al-diopside of the host CAI.

**Discussion:** The  $^{16}\text{O}$ -rich and  $^{16}\text{O}$ -poor reservoirs apparently co-existed during the earliest stages of Solar System evolution [e.g., 19–21]. It has been previously shown that most CAIs in CR2–3, CM2, and CO3.0 chondrites are uniformly  $^{16}\text{O}$ -rich ( $\Delta^{17}\text{O} \sim -23\%$ ) [22–25], indicating formation in a gas of approximately solar composition. In contrast, most CAIs in CCs of petrologic type  $\geq 3.1$  are isotopically heterogeneous: melilite, anorthite, grossite, and some Al,Ti-diopside grains are  $^{16}\text{O}$ -depleted ( $\Delta^{17}\text{O}$  up to  $\sim 0\%$ ) relative to spinel, hibonite, forsterite, and Al-diopside, which are always  $^{16}\text{O}$ -rich ( $\Delta^{17}\text{O} \sim -23\%$ ) [e.g., 22, 25, 26]. The nature of this heterogeneity is controversial: condensation in a gas of variable O-isotope composition and postcrystallization O-isotope exchange in the solar nebular and on the chondrite parent asteroids are being discussed [22, 26–28]. We recently concluded that anorthite, melilite, and grossite in Kaba (CV3.1) and DOM 08004 (CO3.1) CAIs experienced O-isotope exchange with  $^{16}\text{O}$ -poor aqueous fluids on their parent asteroids [25, 26].  $\Delta^{17}\text{O}$  of these fluids are inferred from  $\Delta^{17}\text{O}$  of aqueously-formed fayalite and magnetite in CVs and COs ( $-1.5 \pm 1\%$  and  $-0.2 \pm 0.6\%$ , respectively).

We suggest that the majority of isotopically heterogeneous UR CAIs from CV $\geq 3.1$ s and CO $\geq 3.1$ s we studied originated in an  $^{16}\text{O}$ -rich gas of  $\sim$  solar composition, but subsequently experienced postcrystallization O-isotope exchange with aqueous fluids; some isotopically heterogeneous UR CAIs experienced exchange with an  $^{16}\text{O}$ -depleted nebular gas during chondrule melting. The isotopically homogeneous UR CAIs preserved their original O-isotope compositions, which in most cases, were  $^{16}\text{O}$ -rich. If UR CAI *MUR-1* from Murchison is indeed uniformly  $^{16}\text{O}$ -depleted, it may have originated in an  $^{16}\text{O}$ -depleted gaseous reservoir, similar to an isotopically uniform ( $\Delta^{17}\text{O} \sim -9\%$ ) fine-grained spinel-rich CAI from the CB3.0 chondrite QUE 94627 [29].

**References:** [1] Davis A. (1984) *Meteoritics* 19, 214. [2] Davis A. (1991) *Meteoritics* 26, 330. [3] Weber D. & Bischoff A. (1994) *GCA* 58, 3855. [4] Simon S. et al. (1996) *MAPS* 31, 106. [5] El Goresy A. et al. (2002) *GCA* 66, 1451. [6] Uchiyama K. et al. (2008) *LPS* 39, #1519. [7] Ma C. et al. (2009) *LPS* 40, #1402. [8] Ma C. et al. (2011) *MAPS* 46, A144. [9] Ma et al.

(2011) *LPS* 42, #1276. [10] Ma C. (2011) *MAPS* 46, A144. [11] Ma C. (2012) *MAPS* 47, A256. [12] Ivanova M. et al. (2012) *MAPS* 47, 2107. [13] Ma C. et al. (2013) *Amer. Mineral.* 98, 870. [14] Ma C. et al. (2014) *LPS* 45, #1196. [15] Krot A. et al. (2015) *MAPS* 50, A111. [16] Simon S. & Grossman L. (2015) *MAPS* 31, 106. [17] Makide K. et al. (2013) *GCA* 110, 190. [18] Bischoff A. et al. (2006) in *MESS II*, 679. [19] Yurimoto H. et al. (2006) In *Protostars & Planets V*, 849. [20] Krot A. et al. (2008) *ApJ* 713, 1159. [21] Kööp L. et al. (2016) *GCA* 184, 151. [22] Yurimoto H. et al. (2008) *Rev. Mineral. Geochem.* 68, 141. [23] Makide K. et al. (2009) *GCA* 73, 5018. [24] Kööp L. et al. (2017) *GCA* 189, 70. [25] Simon S. et al. (2017) *LPS* 48, #1083. [26] Krot A. & Nagashima K. (2016) *MAPS* 50, #6104. [27] Aléon et al. (2007) *EPSL* 263, 114. [28] Simon J. et al. (2011) *Science* 331, 1175. [29] Krot A. et al. (2017) *GCA* 201, 155.

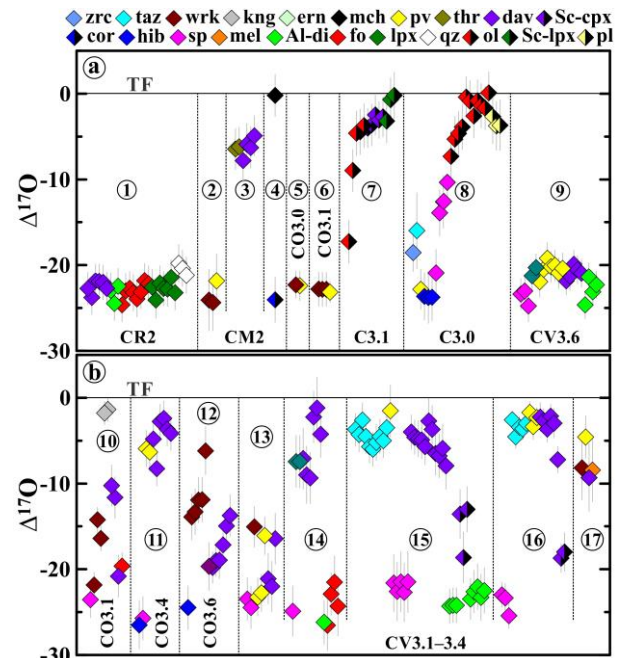


**Fig. 1.**  $\Delta^{17}\text{O}$  of individual minerals in UR CAIs from CCs (1–4 from Y-793261; 2 – *Mur-1*, 3 – *MUR1*, 4 – *UH80-1* from Murchison; 5 – *100* from DOM 08006; 6 – *22-4* from DOM 08004; 7 – *ZZ* from MAC 88107; 8 – *17* from Acfer 094; 9 – *Al-2* from Allende; 10 – *YY* from DOM 08004; 11 – *Oscar* from Ornans; 12 – *Moss-1* from Moss; 13 – *V13*, 14 – *V3* from Vigarano; 15 – *3N-24* from NWA 3118; 16 – *33E* from Efremovka; 17 – *V7* from Vigarano). Al-di = Al-diopside; cor = corundum; dav = davisite; ern = eringaite; grs = grossite; hib = hibonite; kng = kangite; lpx = low-Ca pyroxene; mch = machiite; mel = melilite; ol = Fe-Mg olivine; pl = plagioclase; pv = perovskite; qz = quartz; Sc-px = Sc-rich Al,Ti-diopside (Sc-rich high-Ca pyroxene in 8); sp = spinel (Cr-spinel in 9); taz = tazheranite; thr = thortveitite; wrk = warkite. TF = terrestrial fractionation line. Most UR CAIs from CCs of petrologic type  $\leq 3.1$  are isotopically uniform, except CAIs incompletely melted during chondrule formation (#7, #8, and, possibly, #4). Most UR CAIs of petrologic type  $\geq 3.1$  are isotopically heterogeneous: hibonite, spinel, Al-diopside, and forsterite are always  $^{16}\text{O}$ -rich, whereas warkite, kangite, eringaite, davisite, Sc-rich Al,Ti-diopside, tazheranite, perovskite, and melilite are  $^{16}\text{O}$ -depleted to various degrees.